

## ARTICLE OPEN



# Protection from $\alpha$ -Synuclein induced dopaminergic neurodegeneration by overexpression of the mitochondrial import receptor TOM20

Briana R. De Miranda<sup>1</sup>, Emily M. Rocha<sup>1</sup>, Sandra L. Castro<sup>1</sup> and J. Timothy Greenamyre<sup>1</sup>✉

Dopaminergic neurons of the substantia nigra are selectively vulnerable to mitochondrial dysfunction, which is hypothesized to be an early and fundamental pathogenic mechanism in Parkinson's disease (PD). Mitochondrial function depends on the successful import of nuclear-encoded proteins, many of which are transported through the TOM20–TOM22 outer mitochondrial membrane import receptor machinery. Recent data suggests that post-translational modifications of  $\alpha$ -synuclein promote its interaction with TOM20 at the outer mitochondrial membrane and thereby inhibit normal protein import, leading to dysfunction, and death of dopaminergic neurons. As such, preservation of mitochondrial import in the face of  $\alpha$ -synuclein accumulation might be a strategy to prevent dopaminergic neurodegeneration, however, this is difficult to assess using current in vivo models of PD. To this end, we established an exogenous co-expression system, utilizing AAV2 vectors to overexpress human  $\alpha$ -synuclein and TOM20, individually or together, in the adult Lewis rat substantia nigra to assess whether TOM20 overexpression attenuates  $\alpha$ -synuclein-induced dopaminergic neurodegeneration. Twelve weeks after viral injection, we observed that AAV2-TOM20 expression was sufficient to prevent loss of nigral dopaminergic neurons caused by AAV2- $\alpha$ Syn overexpression. The observed TOM20-mediated dopaminergic neuron preservation appeared to be due, in part, to the rescued expression (and presumed import) of nuclear-encoded mitochondrial electron transport chain proteins that were inhibited by  $\alpha$ -synuclein overexpression. In addition, TOM20 overexpression rescued the expression of the chaperone protein GRP75/mtHSP70/mortalin, a stress-response protein involved in  $\alpha$ -synuclein-induced injury. Collectively, these data indicate that TOM20 expression prevents  $\alpha$ -synuclein-induced mitochondrial dysfunction, which is sufficient to rescue dopaminergic neurons in the adult rat brain.

npj Parkinson's Disease (2020)6:38; <https://doi.org/10.1038/s41531-020-00139-6>

## INTRODUCTION

Among the characteristic molecular pathologies of Parkinson's disease (PD) is the accumulation of  $\alpha$ -synuclein within nigrostriatal dopaminergic neurons. In parallel, these neurons exhibit mitochondrial dysfunction which, in turn, has downstream consequences, including oxidative stress, inflammatory activation, impaired protein trafficking and degradation, and disrupted cellular signaling. Recently, we described a mechanism by which  $\alpha$ -synuclein directly interacts with the mitochondrial translocase of the outer membrane (TOM) receptor, TOM20, and reduces import of proteins which contain an N-terminal mitochondrial targeting signal (MTS)<sup>1</sup>. These data showed that oligomeric, and post-translationally modified  $\alpha$ -synuclein (oxidized, or dopamine modified), but not monomeric or nitrated  $\alpha$ -synuclein, bind to TOM20 and prevent its association with TOM22, a key step in formation of the TOM complex that is necessary for protein import<sup>1</sup>. Because mitochondria must import approximately 99% of the proteins they contain<sup>2,3</sup>, blockade of mitochondrial protein import by toxic species of  $\alpha$ -synuclein may be an early and important contributing factor to dopaminergic neurodegeneration<sup>4,5</sup>.

In rodent studies, overexpression of monomeric wildtype  $\alpha$ -synuclein within the substantia nigra either through viral-mediated expression of SNCA or direct  $\alpha$ -synuclein particle seeding, results in degeneration of dopaminergic neurons and their terminal projections to the striatum<sup>6–8</sup>.  $\alpha$ -Synuclein accumulation and mitochondrial dysfunction are both implicated as mechanisms that contribute to dopaminergic neurodegeneration in PD<sup>4,9–12</sup>. Thus, the interaction between  $\alpha$ -synuclein and TOM20-

mediated protein import may be central to dopaminergic neuron dysfunction and death. Conversely, blocking this mechanism of cellular dysfunction may provide a therapeutic strategy to rescue dopaminergic neurons at an early point in disease pathogenesis.

To this end, we overexpressed human TOM20 in the substantia nigra pars compacta (SNpc) using an adeno-associated (AAV2)-TOM20 vector, injected unilaterally in adult Lewis rats. AAV2-TOM20 was co-expressed with either AAV2-GFP (control) or AAV2- $\alpha$ Syn. Similar to previous reports, AAV2- $\alpha$ Syn treatment caused significant loss of dopaminergic neurons following 12 weeks of viral incubation, and surviving cells contained both soluble and insoluble  $\alpha$ -synuclein aggregates that correspond to human Lewy pathology<sup>13–15</sup>. Co-expression of AAV2-TOM20 with AAV2- $\alpha$ Syn did not reduce  $\alpha$ -synuclein expression or accumulation within cells of the SNpc, however, it did result in neuroprotection against dopaminergic cell death. In conjunction, AAV2-TOM20 treatment rescued the expression of nuclear-encoded proteins in this in vivo, proof-of-principal study examining the interaction of  $\alpha$ -synuclein and mitochondrial function within dopaminergic neurons.

## RESULTS

Characterization of AAV2-mediated TOM20 and  $\alpha$ -synuclein overexpression

Adult (10-month-old) male Lewis rats were randomly assigned into three treatment groups and received a combination of two AAV2 viral vectors: AAV2-TOM20/GFP (control), AAV2- $\alpha$ Syn/GFP

<sup>1</sup>Pittsburgh Institute for Neurodegenerative Diseases and Department of Neurology, University of Pittsburgh, Pittsburgh, PA, USA. ✉email: [jgreena@pitt.edu](mailto:jgreena@pitt.edu)

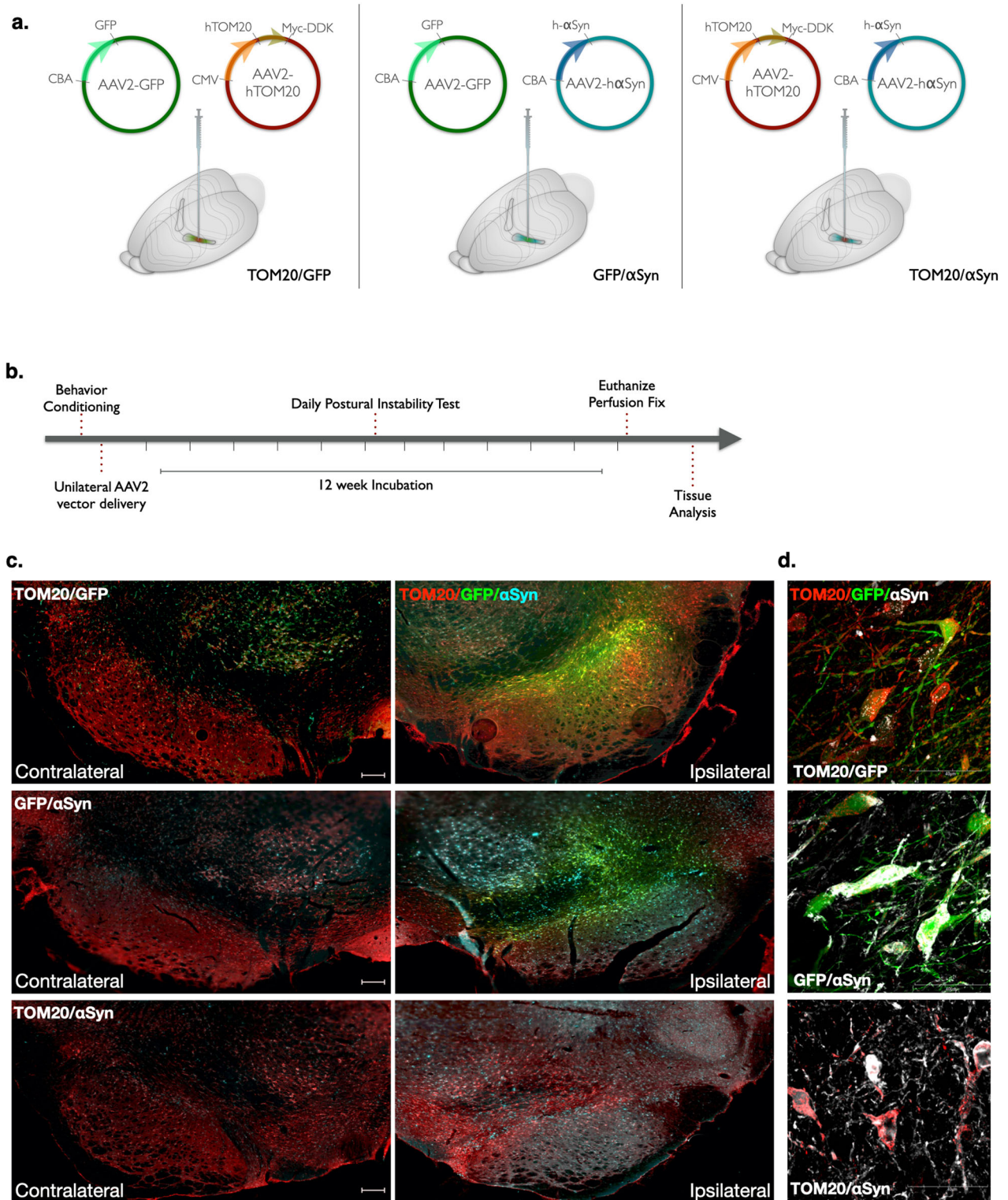


**Fig. 1** AAV2-mediated expression of human TOM20 and  $\alpha$ Syn in the rat midbrain. AAV2 vectors driving protein overexpression were injected via stereotaxic surgery into the right substantia nigra of adult, male Lewis rats. Vector combinations of AAV2-TOM20/GFP, AAV2- $\alpha$ Syn/GFP, and AAV2-TOM20/ $\alpha$ Syn represent the three treatment groups utilized within this study (**a**). Following vector infusion, animals were monitored daily for motor behavior, and euthanized for tissue collection 12-weeks post-injection (**b**). Representative images from each vector treatment group comparing ipsilateral (injected) and contralateral (non-injected) brain hemispheres; TOM20 (red),  $\alpha$ Syn (cyan), GFP (green); scale bar 100  $\mu$ m (**c**). Target protein overexpression in neurons 12 weeks following vector expression; TOM20 (red),  $\alpha$ Syn (white), GFP (green; **d**).

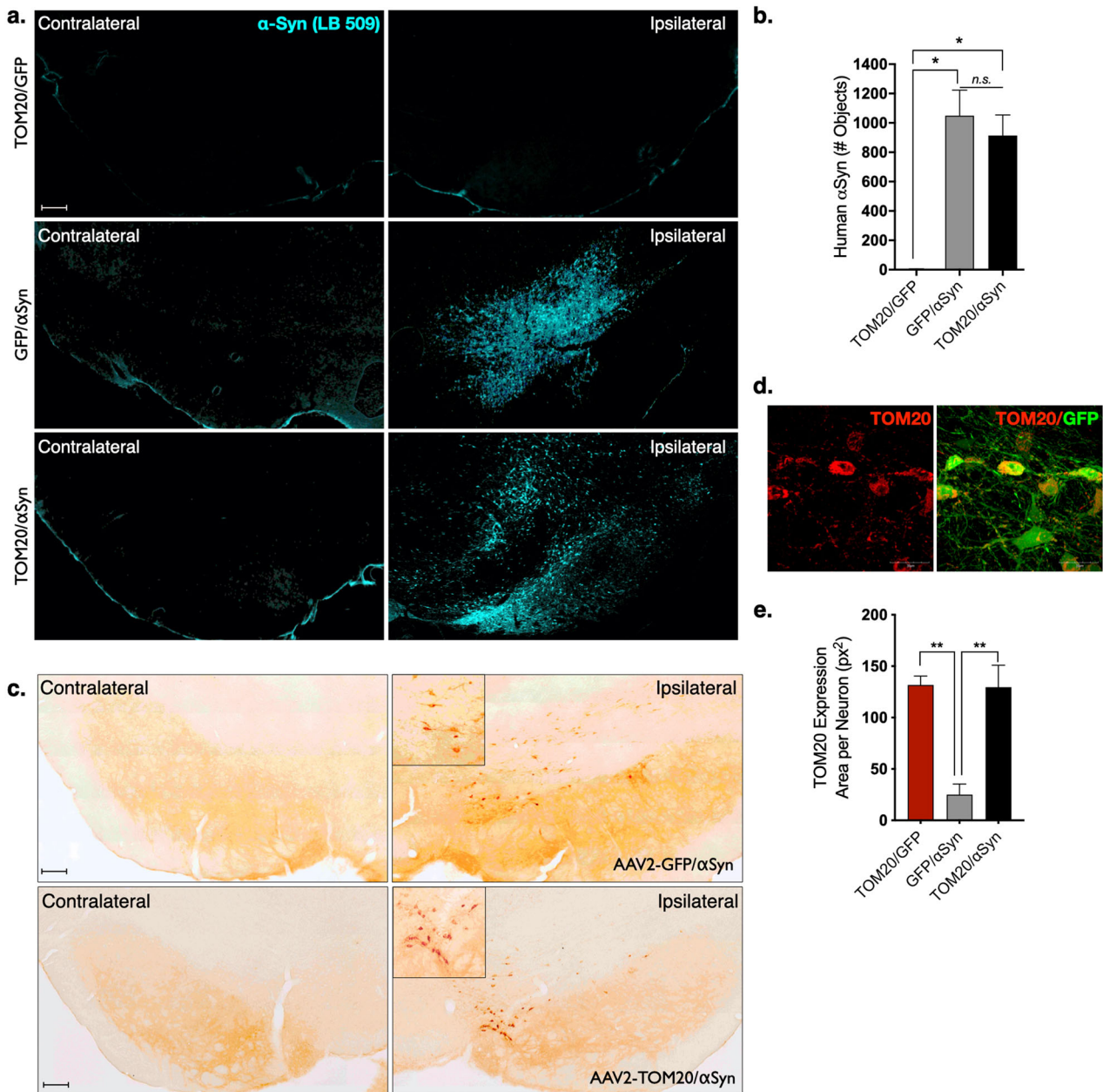


**Fig. 2** Vector co-administration does not substantially alter target protein expression. Human αSyn protein expression was detectable within the injected hemisphere of AAV2-αSyn/GFP and AAV2-TOM20/αSyn and was expressed at similar levels in both treatment groups receiving the human αSyn vector; ( $F(2, 26 = 4.6)$ ,  $p = 0.0192$ , ANOVA); scale bar 100 μm (a, b). Insoluble αSyn (proteinase K resistant) was confirmed in animals injected with AAV2-αSyn vectors; representative image from AAV2-TOM20/αSyn; scale bar 100 μm (c). AAV2-TOM20 vector infusion resulted in significantly elevated levels of TOM20 within neurons of the ventral midbrain, which was not affected by co-expression of AAV2-αSyn; ( $F(2, 6 = 17.5)$ ,  $p = 0.0031$ , ANOVA; d, e). Error bars depict standard error of the mean (s.e.m.).

(disease control), or AAV2-TOM20/αSyn (Fig. 1a and Supplemental Fig. 1). Following vector infusion, animals were monitored over a 12-week period, previously established for maximum AAV2-mediated α-synuclein expression to occur (Fig. 1b)<sup>16</sup>. Midbrain histological analyses revealed a robust protein overexpression with each viral vector (human TOM20, GFP, or human αSyn) in the substantia nigra ipsilateral to the stereotactic injection (Fig. 1c, d).

Animals that received AAV2-αSyn/GFP or AAV2-TOM20/αSyn injections displayed a robust expression of human α-synuclein protein with the neurons of the substantia nigra, which was absent in the AAV2-TOM20/GFP control group (Fig. 2a, b). Midbrain tissue from animals expressing human AAV2-TOM20/αSyn was incubated with proteinase K, which revealed a fraction of insoluble α-

synuclein protein aggregates following 12 weeks of viral vector incubation within the ipsilateral injection hemisphere (Fig. 2c). Animals receiving AAV2-TOM20/GFP or AAV2-TOM20/αSyn vectors expressed approximately 5-fold increase of TOM20 protein within dopaminergic neuron cell bodies (positive for tyrosine hydroxylase; TH) compared to animals that did not receive the TOM20 overexpression vector (AAV2-αSyn/GFP; Fig. 2d, e).

Vector-infused animals were assayed for motor behavioral changes during the 12-week incubation period using a postural instability test to identify unilateral motor movement deficits. Postural instability testing (PIT) revealed no significant difference between treatment groups over the course of the study (Supplemental Fig. 2a). A cylinder test was performed at the end

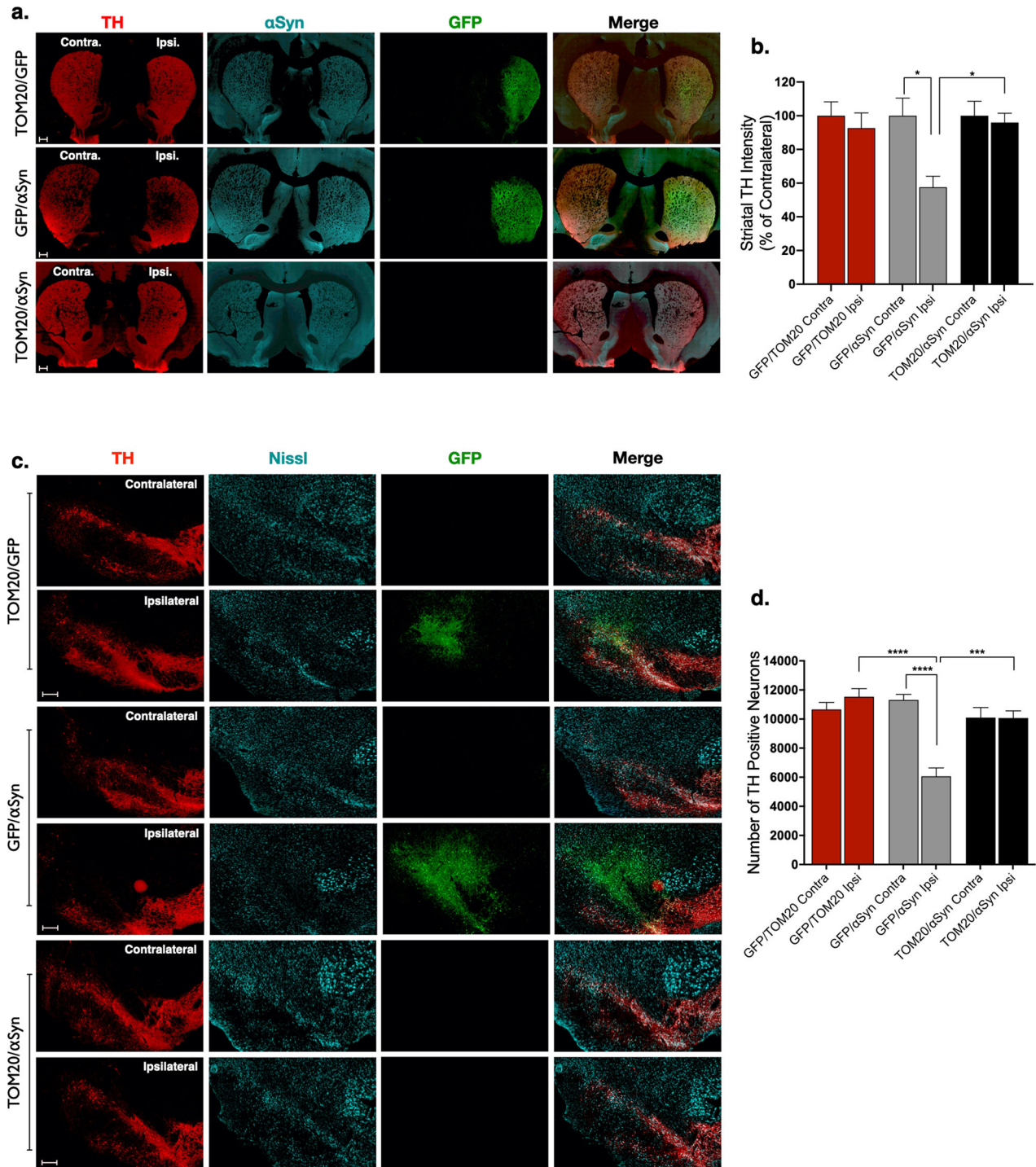
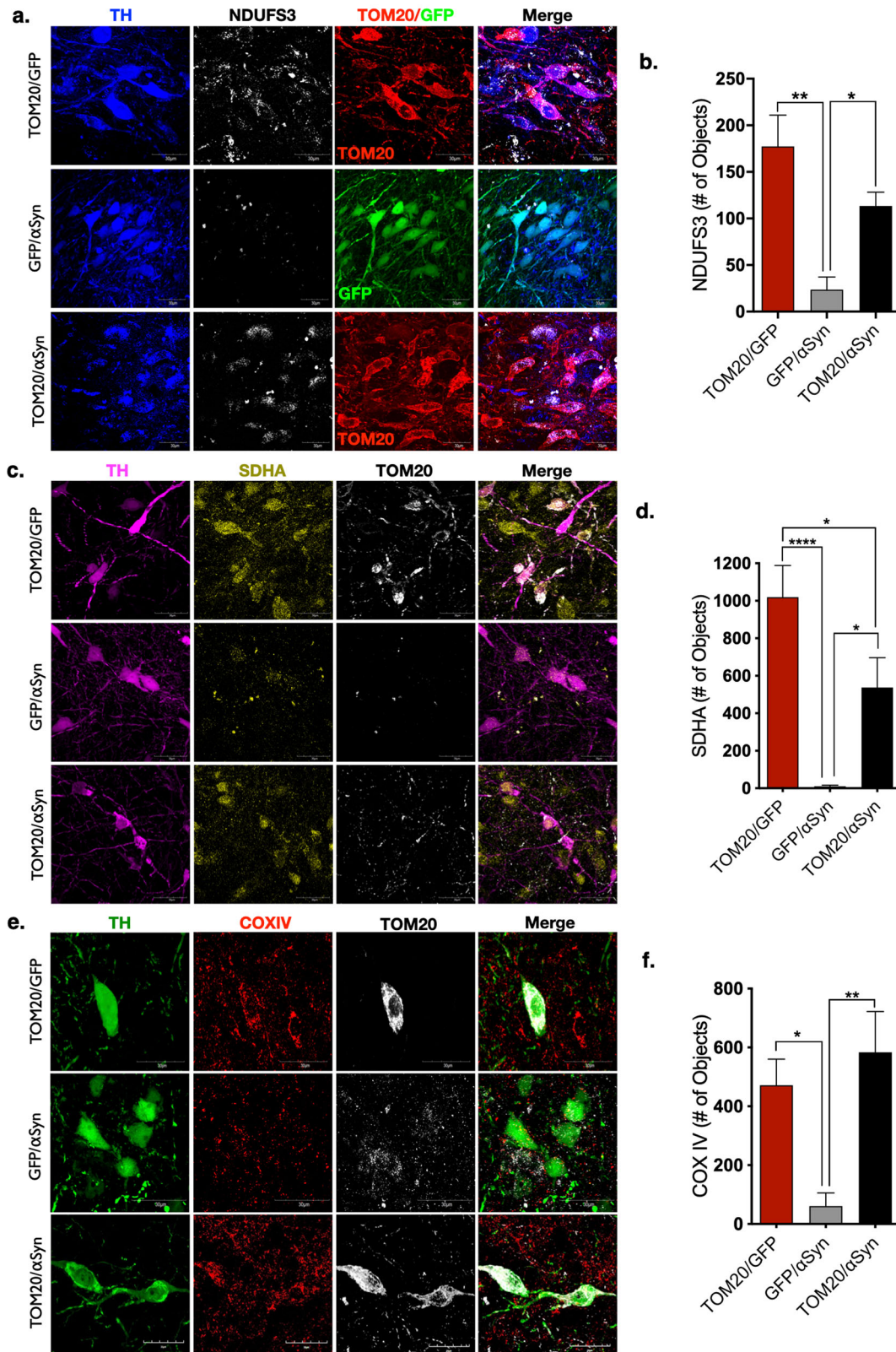


**Fig. 3 Overexpression of TOM20 was neuroprotective against AAV2- $\alpha$ Syn-mediated dopaminergic neurodegeneration.** Dopaminergic terminals within the striatum (tyrosine hydroxylase; TH; red) were significantly reduced compared to the contralateral side in animals expressing AAV2- $\alpha$ Syn/GFP, but not in animals expressing AAV2-TOM20/ $\alpha$ Syn; TH (red),  $\alpha$ Syn (cyan), GFP (green); (F(5, 95 = 3.0),  $p = 0.0146$ , ANOVA; **a, b**). Representative images from the ipsilateral and contralateral hemispheres of each treatment group show significant dopaminergic neuron loss (TH, red) following AAV2- $\alpha$ Syn/GFP treatment, which was reduced by co-expression with TOM20 (AAV2-TOM20/ $\alpha$ Syn); (F(5, 20 = 12.07),  $p < 0.0001$ , ANOVA); scale bars 100  $\mu$ m (**c, d**). Error bars depict standard error of the mean (s.e.m.).

of the 12-week incubation period; however, neither the total number of rears nor preferential paw placement (percent paw asymmetry) was significantly affected by  $\alpha$ -synuclein or TOM20 overexpression (Supplemental Fig. 2b, c). Similarly, no significant morbidity was observed in any treatment group during the 12-week time course of the study.

TOM20 overexpression is protective against  $\alpha$ -synuclein-induced neurodegeneration

Striatal brain sections from injected animals were assessed for TH-positive terminal density and compared to the contralateral uninjected hemisphere. Animals receiving AAV2- $\alpha$ Syn/GFP vectors had ~40% reduced TH fiber density ipsilateral to virus injection



( $p = 0.0186$ ), and this was prevented in animals that received TOM20 overexpression vector in conjunction with  $\alpha$ -synuclein (AAV2-TOM20/ $\alpha$ Syn; Fig. 3a, b). Similarly, dopaminergic neurons within the SNpc were significantly depleted (47% loss) by AAV2-mediated overexpression of  $\alpha$ -synuclein (AAV2- $\alpha$ Syn/GFP;

Fig. 3c, d); however, co-expression with TOM20 protected against  $\alpha$ -synuclein-induced dopaminergic neuron cell death ( $p < 0.0001$ ; AAV2-TOM20/ $\alpha$ Syn). Thus, at the level of both the terminals and the cell bodies, TOM20 overexpression provided protection against  $\alpha$ -synuclein.

**Fig. 4 TOM20 expression rescued nuclear encoded mitochondrial protein expression impaired by  $\alpha$ Syn.** NADH:Ubiquinone Oxidoreductase Core Subunit S3 (NDUFS3, white) is a component of complex I of the electron transport chain. NDUFS3 expression is significantly reduced in dopaminergic neurons of animals expressing AAV2- $\alpha$ Syn/GFP, and rescued by AAV2-TOM20 co-expression; TOM20 (red), GFP (green), TH (blue); (F(2, 10 = 11.82),  $p = 0.0023$ , ANOVA; **a, b**). Succinate dehydrogenase complex flavoprotein subunit A (SDHA, yellow) encodes the catalytic subunit of succinate-ubiquinone oxidoreductase of the electron transport chain, was reduced within mitochondria of dopaminergic neurons following  $\alpha$ Syn overexpression, and rescued by AAV2-TOM20 co-expression; TOM20 (white), TH (magenta); (F(2, 23 = 14.57),  $p = 0.0001$ , ANOVA; **c, d**). Cytochrome c oxidase or complex IV (COX IV, red) the final enzyme in the mitochondrial transport chain, displayed a significant reduction within mitochondria in dopaminergic neurons expressing AAV2- $\alpha$ Syn/GFP, but not neurons expressing AAV2-TOM20/ $\alpha$ Syn; TOM20 (red), TH (green); (F(2, 23 = 8.46),  $p = 0.0018$ , ANOVA; **e, f**). Error bars depict standard error of the mean (s.e.m.).

Nuclear encoded mitochondrial protein expression impaired by  $\alpha$ -synuclein is preserved by AAV2-TOM20

To determine whether TOM20 overexpression resulted in functional restoration of mitochondrial protein expression, we assayed for nuclear encoded electron transport chain (ETC) proteins imported through the TOM20–TOM22 complex: NADH:Ubiquinone Oxidoreductase Core Subunit S3 (NDUFS3), succinate dehydrogenase [ubiquinone] flavoprotein subunit, mitochondrial (SDHA), and cytochrome c oxidase/complex IV (COX-IV). Following vector infusion, dopaminergic neurons in the SN that were transduced with AAV2- $\alpha$ Syn/GFP expressed significantly reduced protein levels of NDUFS3 (86% loss;  $p < 0.01$ ), SDHA (90% loss;  $p < 0.0001$ ), and COX-IV (85% loss;  $p < 0.05$ ), compared to transduced neurons in AAV2-TOM20/GFP-injected animals (Fig. 4a–f). In contrast, dopaminergic neurons that overexpressed both  $\alpha$ -synuclein and TOM20 (AAV2-TOM20/ $\alpha$ Syn) showed preserved expression of NDUFS3 ( $p < 0.05$ ), SDHA ( $p < 0.01$ ), and COX-IV ( $p < 0.05$ ).

The expression of mitochondrial protein GRP75/mtHSP70 is stress-responsive

Another nuclear-encoded mitochondrial protein, GRP75/mtHSP70 (mortalin), is both imported through the TOM20–TOM22 channel and is reportedly upregulated in response to mitochondrial oxidative stress, which can be caused by  $\alpha$ -synuclein toxicity<sup>4,17</sup>. Unlike the imported ETC proteins, mitochondrial expression GRP75 was not significantly affected by  $\alpha$ -synuclein overexpression (30% loss;  $p = 0.5$ ), however, the combined expression of  $\alpha$ -synuclein and TOM20 (AAV2-TOM20/ $\alpha$ Syn) caused a robust increase in GRP75 (5-fold increase;  $p < 0.0001$ ) that colocalized with TOM20 in dopaminergic neurons (Fig. 5a, b). These data suggest that GRP75 imparts an important protective function in mitochondria damaged by  $\alpha$ -synuclein accumulation, but GRP75 localization within the mitochondria is dependent on functional TOM20 import machinery.

To further investigate the stress-dependent response of GRP75 import into the mitochondria, we treated adult male Lewis rats with neurotoxin and prototypical complex I inhibitor rotenone, which results in significant mitochondrial dysfunction within dopaminergic neurons, including impaired protein import<sup>1,18,19</sup>. Animals were given a daily intraperitoneal (i.p.) rotenone injection (2.8 mg/kg) over an acute time course (5 days), which results in a marked oxidative stress response, and the accumulation of endogenous  $\alpha$ -synuclein within dopaminergic neurons, but does not cause dopaminergic neurodegeneration<sup>15</sup>. A separate cohort of adult male Lewis rats were administered “endpoint” or chronic rotenone treatment, in which animals are given a daily injection of rotenone (2.8 mg/kg) until they exhibit predefined motor-behavioral impairment, which coincides with dopaminergic neuron death in the substantia nigra<sup>20–22</sup>. Acute (5 Day ROT) treatment resulted in a significant increase in GRP75 protein within dopaminergic neurons of the SN ( $p = 0.0011$ ), but GRP75 expression was significantly decreased ( $p = 0.001$ ) in dopaminergic neurons of animals receiving chronic rotenone treatment (Endpoint ROT; Fig. 5c, d). Thus, elevated expression of GRP75 appears to be an early, possibly compensatory, response to mitochondrial stress, which cannot be sustained with prolonged

or ongoing impairment, likely because of dysfunctional import into mitochondria.

## DISCUSSION

Post-translational modification (PTM) and oligomerization of  $\alpha$ -synuclein are implicated in the mitochondrial dysfunction that may precede dopaminergic neurodegeneration in PD<sup>1</sup>. These “toxic” forms of the protein have been observed in postmortem brain tissue of individuals with idiopathic PD using assays for oligomeric<sup>23</sup> and phosphorylated forms of  $\alpha$ -synuclein<sup>12,24</sup>. In this context, we previously reported that oligomeric or PTM forms of  $\alpha$ -synuclein bind to the TOM20 subunit of the TOM20–TOM22 import complex and block mitochondrial protein import, a process which we proposed could be a possible target for therapeutic intervention to prevent dopaminergic neurodegeneration in PD<sup>1</sup>. To this end, we have utilized a viral vector-mediated model of human  $\alpha$ -synuclein overexpression in the SN of adult Lewis rats to reproduce accumulation of  $\alpha$ -synuclein protein within dopaminergic neurons. By coexpressing TOM20 together with  $\alpha$ -synuclein, we attempted to ameliorate impaired mitochondrial protein import deficits and thereby rescue dopaminergic neurons from  $\alpha$ -synuclein-induced neurodegeneration. Our results confirm that  $\alpha$ -synuclein overexpression causes nigrostriatal dopaminergic neurodegeneration, which is associated with loss of nuclear-encoded mitochondrial proteins<sup>1</sup>. Here, we report the novel in vivo finding that TOM20 overexpression restores levels of nuclear-encoded mitochondrial proteins, even in the face of continued  $\alpha$ -synuclein overexpression, and protects these neurons against degeneration.

The mitochondrial genome encodes only 13 of the roughly 1300 proteins contained in the organelle. Therefore, mitochondria depend on specific import mechanisms to acquire 99% of their protein constituents<sup>25</sup>. Levels of inner membrane/matrix respiratory chain components essential for proper mitochondrial function, such as the iron–sulfur subunit of complex I, NDUFS3, the complex IV subunit, COXIV, and the complex II flavoprotein subunit, SDHA, were all markedly reduced by  $\alpha$ -synuclein overexpression—and this was associated with nigrostriatal degeneration. In contrast, the combined expression of exogenous TOM20 with  $\alpha$ -synuclein largely prevented the loss of nuclear encoded protein expression and protected against  $\alpha$ -synuclein toxicity. The survival of SN neurons co-expressing TOM20 with  $\alpha$ -synuclein indicates that sustained expression of the mitochondrial protein import machinery was sufficient to protect against  $\alpha$ -synuclein-induced dopaminergic neuron death.

Nuclear-encoded proteins destined for mitochondrial import via the TOM20–TOM22 system contain an MTS, also known as a presequence<sup>26</sup>. Such proteins are guided through the inner membrane to the matrix by the translocase of the inner membrane import channel in concert with the matrix chaperone, mtHSP70 (GRP75/mortalin), to maintain proteins in an unfolded state as they are processed by the mitochondrial processing peptidase (MPP)<sup>27</sup>. The function of GRP75 is pleiotropic; it is involved in protein import, but also plays a

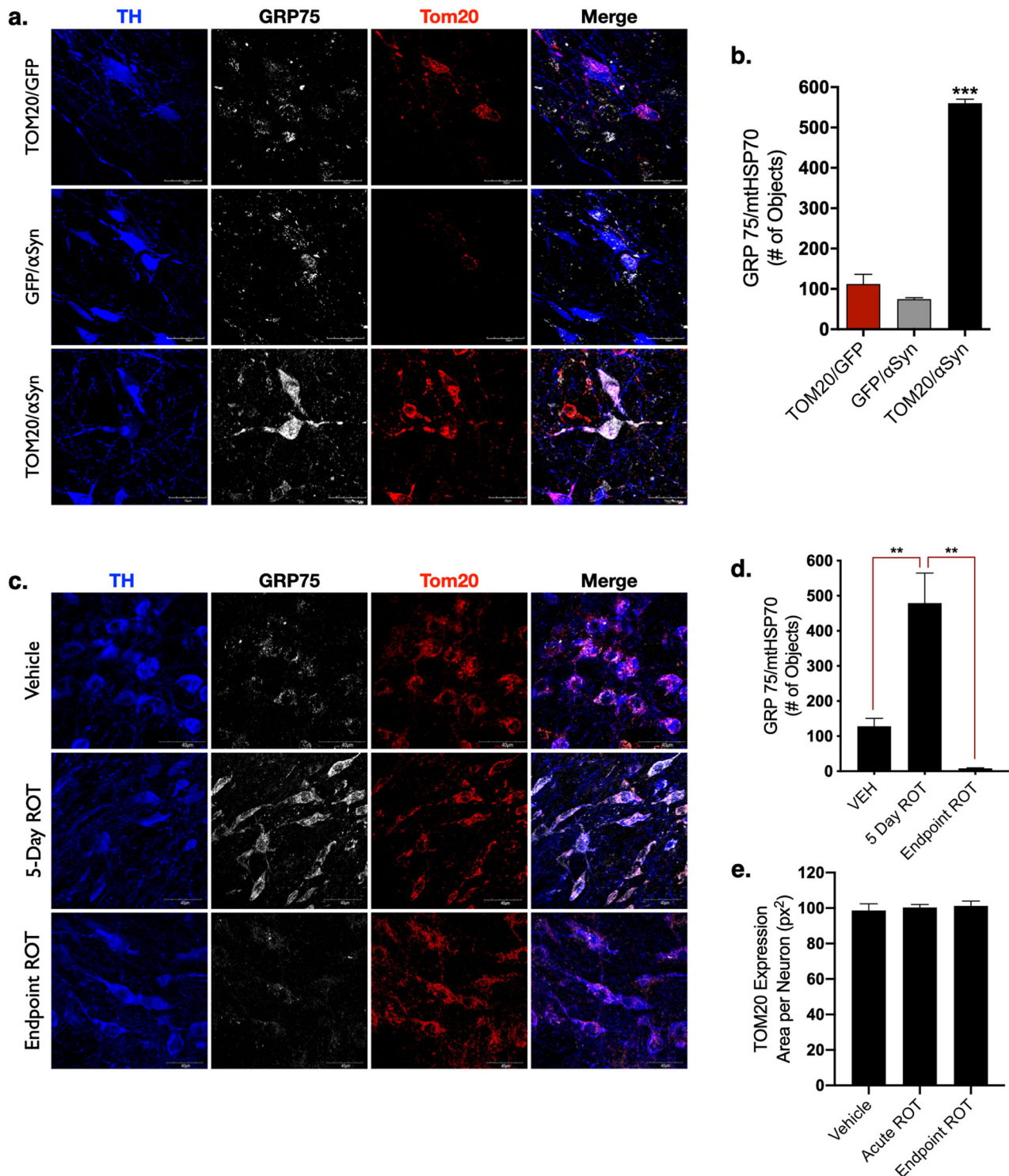


**Fig. 5** GRP75 expression is influenced by  $\alpha$ Syn, TOM20, and the mitochondrial toxicant rotenone. The redox-sensitive mitochondrial chaperone protein GRP75 was significantly elevated in dopaminergic neurons expressing AAV2-TOM20/ $\alpha$ Syn, but not AAV2- $\alpha$ Syn/GFP, or AAV2-TOM20/GFP; ( $F(2, 4 = 167.2)$ ,  $p = 0.0001$ , ANOVA; **a, b**). Acute rotenone treatment causes the endogenous accumulation of  $\alpha$ Syn (5-day ROT) that corresponded to a significant elevation in GRP75 expression within mitochondria, which was diminished in chronic/endpoint rotenone treated rats; ( $F(2, 15 = 14.69)$   $p = 0.0003$ , ANOVA; **c, d**). Total TOM20 protein expression in the dopaminergic neurons of the SN was not significantly changed following rotenone treatment (**e**). Error bars depict standard error of the mean (s.e.m.).

role in mitochondria-endoplasmic reticulum (ER) coupling<sup>28</sup>, where it appears to regulate  $\text{Ca}^{2+}$  transfer through the mitochondria-associated membrane (MAM). GRP75 has been implicated in the pathogenesis of PD, and was shown to be decreased in the postmortem brain tissue, and serum of

individuals with PD compared to age-matched controls<sup>29,30</sup>. Reduced GRP75 function in dopaminergic neurons appears to impair mitochondrial quality control, and induces Parkin-mediated mitophagy resulting in depletion of total cellular mitochondria<sup>31</sup>.

The robust GRP75 signal seen in dopaminergic neurons from animals co-expressing exogenous  $\alpha$ -synuclein and TOM20—but neither control nor  $\alpha$ -synuclein-overexpressing animals—indicates that (i) GRP75 is upregulated in response to  $\alpha$ -synuclein induced stress, and (ii) expression of this chaperone protein also requires functional mitochondrial import. This is further corroborated by our finding of elevated levels of GRP75 with acute rotenone, but dramatic loss of GRP75 with chronic rotenone exposure, at a time when mitochondrial import is known to be impaired<sup>1</sup>. As a multifunctional, redox sensitive protein, reduced GRP75 expression in dopaminergic neurons from  $\alpha$ -synuclein overexpression or rotenone exposure may contribute to several pro-death pathways, including calcium dysregulation<sup>32</sup>, energy deprivation<sup>33</sup>, and apoptotic signaling<sup>34</sup>.

Impairment of protein import into the mitochondria extends beyond imported electron transport chain proteins, as the proteins required for maintenance of mitochondrial DNA (mtDNA) are also nuclear-encoded and likewise depend on the import machinery<sup>26</sup>. In addition, oxidative stress, whether toxicant or  $\alpha$ -synuclein-induced, produces mtDNA damage<sup>35</sup>, which is known to elicit specific vulnerability to dopaminergic neurons<sup>36,37</sup>. The markers of mitochondrial dyshomeostasis observed within surviving cells following  $\alpha$ -synuclein overexpression in this model suggests multiple, likely feed-forward, mechanisms surrounding mitochondrial protein import ultimately contribute to the death of dopaminergic neurons. Conversely, the overexpression of TOM20 provided sustained expression of elements key to mitochondrial homeostasis within dopaminergic neurons.

There were limitations of this study. The experimental design focused on histological outcomes; as such, the use of fixed tissue precluded assays of mitochondrial function and dynamics within dopaminergic neurons. Additionally, we found no behavioral deficits associated with  $\alpha$ -synuclein overexpression and could therefore not measure improvement with TOM20 overexpression. This lack of a gross motor phenotype was most likely a result of the combination of a slowly evolving lesion (with ongoing compensation) and the moderate final level of nigrostriatal degeneration (~40%). In contrast with other  $\alpha$ -synuclein overexpression studies<sup>7,38</sup> the use of middle-aged (10-month-old) rats may have limited motor phenotype measurement, as older rats tend to exhibit lower physical performance in behavioral assays<sup>39</sup>. As aging is the predominant risk factor in PD development<sup>40</sup>, aged, rather than young adult rats, were strategically utilized in this study for both AAV2 and rotenone treatment.

Collectively, however, these data show that  $\alpha$ -synuclein overexpression in dopaminergic neurons of the adult SN impairs nuclear encoded mitochondrial protein expression and causes neurodegeneration. TOM20 overexpression was sufficient to rescue  $\alpha$ -synuclein-induced dopaminergic neurodegeneration over this 12-week time period, likely because it improved mitochondrial function<sup>1</sup>, which is integral to dopaminergic neuron survival<sup>41–43</sup>. Additionally, these data suggest a role for the mitochondrial chaperone and redox sensitive protein, GRP75/mtHSP70, in protection of dopaminergic neurons from  $\alpha$ -synuclein induced pathology. Although multiple mechanisms of toxicity have been ascribed to  $\alpha$ -synuclein, our finding of virtually complete neuroprotection with TOM20 overexpression indicates that its interactions with mitochondria may be a major means by which it causes

neurodegeneration. As such, the  $\alpha$ -synuclein–TOM20 interaction may represent an important target for therapeutic intervention.

## METHODS

### Adeno-associated viral vectors

Viral vectors were utilized to overexpress GFP, human wild type  $\alpha$ -synuclein, or human TOM20. Each vector was expressed in an adeno-associated virus (serotype AAV2). The AAV2-TOM20 vector was produced by the Gene Therapy Program of the University of Pennsylvania Vector Core Program (Philadelphia, PA). AAV2- $\alpha$ Syn and AAV2-GFP vectors were purchased from the University of North Carolina Vector Core, through a partnership with the Michael J. Fox Foundation. Vector information is listed in Table 1.

### Chemical reagents and supplies

Chemicals were purchased from Sigma-Aldrich (St. Louis, MO) unless otherwise noted. Antibodies are listed in Table 2.

### Stereotaxic rodent surgery

Adult, middle age (10 month), male Lewis rats (Envigo, Indianapolis, IN) were utilized for AAV2 vector delivery. Middle-aged Lewis rats, rather than young adult animals, were selected for this study as aging is the most significant risk factor in PD development. Animals were maintained under standard temperature and humidity-controlled conditions with 12:12 h light-dark cycle. Conventional diet and water were provided ad libitum. Rats were randomly assigned to each treatment group and given a four-digit code following surgery to blind researchers.

Rodent stereotaxic surgery was performed under deep isoflurane anesthesia. Each animal received a unilateral infusion of two AAV2 vectors simultaneously (1  $\mu$ l per vector, total of 2  $\mu$ l); (1) GFP and TOM20, (2) GFP and  $\alpha$ Syn, or (3)  $\alpha$ Syn and TOM20, using standard Bregma coordinates for the substantia nigra (Bregma  $-5.8$  mm A/P,  $-2.2$  mm M/L, and  $-8.5$  mm V). Postoperative care included daily analgesic buprenorphine injections for three days following surgery, and sutures were removed upon wound closure. Animals were single-housed for the entirety of the 12-week study period, and euthanized using a lethal dose of pentobarbital, followed by transcardial perfusion with PBS and 4% paraformaldehyde perfusion fixation. All experiments involving animal treatment and euthanasia were approved by the University of Pittsburgh Institutional Animal Care and Use Committee.

### Motor behavior analysis

Prior to stereotaxic surgery, animals were habituated to the postural instability test (PIT), and daily handling. PIT was used to assess asymmetric motor function, and is described in detail by Woodlee et al.<sup>44</sup>. Briefly, each animal was held vertically with one forelimb allowed to contact the table surface, which was lined with medium grit sandpaper. The animal's center of gravity was then advanced until the animal triggered a "catch-up" step. The distance (cm) required for the animal to regain the center of gravity was recorded. Three trials were assessed per forelimb at each timepoint, and the average distance for each trial was recorded. PIT was assessed weekly for contralateral and ipsilateral forelimbs three weeks prior to surgery, and for 12-weeks postvector infusion. Cylinder test recording was conducted at week 12; animals were placed in a glass cylinder (diameter 14 inches) and recorded for five continuous minutes in a closed environment. Behavioral tests were carried out by investigators blinded to treatment group throughout the study.

**Table 1.** Vector information.

Protein expression	Vector description	Species	Titer (GC/mL)	Injection Volume	Source
TOM20	AAV2.CMV.PI.TOM20.WPRE.bGH (p3863)	Human	8.6e12	1 $\mu$ l	Penn Vector Core
$\alpha$ Syn	AAV2.CBA. $\alpha$ -synuclein	Human	1.5e13	1 $\mu$ l	UNC Vector Core
GFP	AAV2.CBA.eGFP	Aequorea victoria	8.1e12	1 $\mu$ l	UNC Vector Core



**Table 2.** Antibody information.

Antibody	Catalog	Tissue concentration	Company
Tyrosine hydroxylase	AB1542	1:2000	EMD Millipore (Burlington, MA)
Human- $\alpha$ -Synuclein (LB509)	Ab 27766	1:1000	Abcam (Cambridge, MA)
COX-IV	Ab16056	1:500	
GRP75/mtHSP70	Ab2799	1:500	
TOM20 (Ms)	612278	1:500	BD Biosciences (San Jose, CA)
$\alpha$ -Synuclein (total)	610787	1:500	
NDUFS3/OxPhos	459130	1:500	Thermo Fisher (Waltham, MA)
TOM20 (Rb)	SC-11415	1:500	Santa Cruz Biotechnology (Santa Cruz, CA)
SDHA	NBP1-71688	1:500	Novus Biologicals (Centennial, CO)

### Rotenone administration

Adult (10 month) male Lewis rats (Envigo) were separated into single-housing, and handled for two weeks prior to the onset of rotenone administration. Rotenone was dissolved in DMSO (2% final concentration) and Miglyol 812 to reach the final concentration of 2.8 mg/kg. Rotenone handling and disposal was carried out following University of Pittsburgh Environmental Health and Safety procedures. Acute (5 Day ROT), endpoint rotenone (Endpoint ROT) and vehicle (2% DMSO and Miglyol) groups were randomly divided, and each animal was administered a single daily intraperitoneal (*i.p.*) injection of rotenone for 5 days (acute) or until they reached their motor behavioral endpoint, defined by the inability to perform the postural instability test or loss of 25% body mass.

### Striatal terminal intensity

Coronal rat brain sections (35  $\mu$ m) encompassing the volume of the rat striatum (1/6 sampling fraction, approximately ten sections per animal) were stained for tyrosine hydroxylase (TH) and detected using an infrared secondary antibody (IRDye<sup>®</sup> 680, LiCor Biosciences). Striatal tissue sections were analyzed using near-infrared imaging for density of dopamine neuron terminals (LiCor Odyssey) and analyzed using LiCor Odyssey software (V3.0; Licor Biosciences, Lincoln, NE). Output for striatal TH intensity is arbitrary fluorescence units.

### Stereology

Stereological analysis of dopamine neuron number in the SN was achieved using an adapted protocol from Tapias et al.<sup>45</sup> and Tapias and Greenamyre<sup>46</sup> as reported in De Miranda et al.<sup>20,47</sup> employing an unbiased, automated system as an alternative to the optical fractinator method. Briefly, 35  $\mu$ m coronal nigral tissue sections (1/6 sampling fraction encompassing the volume of the entire SN) were stained for TH and counterstained with DAPI and NeuroTrace Dye (640; Life Technologies) and imaged using a Nikon 90i upright fluorescence microscope equipped with high N.A. plan fluor/apochromat objectives, Renishaw linear encoded microscope stage (Prior Electronics) and Q-imaging Retiga cooled CCD camera (Center for Biological Imaging, University of Pittsburgh). Images were processed using Nikon NIS-Elements Advanced Research software (Version 4.5, Nikon, Melville, NY), and quantitative analysis was performed on fluorescent images colocalizing DAPI, TH, and Nissl-positive stains. Results are reported as the number of TH-positive cell bodies (whole neurons) within the SN.

### Immunohistochemistry and pathology

Brain sections (35  $\mu$ m) were maintained at  $-20^{\circ}\text{C}$  in cryoprotectant, stained while free-floating, and mounted to glass slides for imaging, using a "primary antibody delete" (secondary antibody only) stained section to establish background fluorescence limits. Fluorescent immunohistochemical images were collected using an Olympus BX61 confocal microscope and Fluoview 1000 software (Melville, NY). Quantitative fluorescence measurements were thoroughly monitored using standard operating imaging parameters to ensure that images contained no saturated pixels. For quantitative comparisons, all imaging parameters (e.g., laser power, exposure, and pinhole) were held constant across specimens. Confocal images were analyzed using Nikon NIS-Elements Advanced Research software (Version 4.5, Nikon, Melville, NY). A minimum of six images per tissue slice were analyzed per animal, averaging 9–15 neurons per 60–100 $\times$  image (approximately 180 cells per animal, per histological stain). 20 $\times$  magnification was used to generate montage imaging of the ventral midbrain, for which the entire SN was analyzed per image using anatomical region of interest (ROI) boundaries. Results are reported as a measure of puncta within TH-

positive cells, either number of objects (# of objects), or area per neuron in square pixels ( $\text{px}^2$ ), generated by Nikon Elements Advanced Research software.

### Statistical analysis

An a priori power analysis was conducted to determine the minimal number of animals required to achieve 20–40% variance of the mean, with a 95% power at  $\alpha = 0.05$  using G\*Power statistical software ( $N = 5$  per group). All data were expressed as mean values  $\pm$  standard error of the mean (s.e.m.). Statistical significance was evaluated between normally distributed means by parametric one-way analysis of variance (ANOVA) with the Tukey post-hoc test to compare multiple data sets, or an unpaired *t*-test comparison of two means. Statistical significance is represented in each Figure as \* $p < 0.05$ , \*\* $p < 0.01$ , \*\*\* $p < 0.001$ , \*\*\*\* $p < 0.0001$ , unless otherwise specified on graph. *F* and *T* statistics are reported in each figure legend for ANOVA and *t*-tests, respectively. Postural instability was evaluated using the Kruskal–Wallis test ( $p < 0.05$ ). Statistical analyses were carried out using GraphPad Prism software (V. 8.3.0).

### Reporting summary

Further information on research design is available in the Nature Research Reporting Summary linked to this article.

### DATA AVAILABILITY

The data that support the findings of this study are available from the corresponding author on reasonable request.

Received: 12 May 2020; Accepted: 21 October 2020;

Published online: 08 December 2020

### REFERENCES

- Di Maio, R. et al.  $\alpha$ -Synuclein binds to TOM20 and inhibits mitochondrial protein import in Parkinson's disease. *Sci. Transl. Med.* **8**, 342ra78–342ra78 (2016).
- Anderson, S. et al. Sequence and organization of the human mitochondrial genome. *Nature* **290**, 457–465 (1981).
- Andrews, R. M. et al. Reanalysis and revision of the Cambridge reference sequence for human mitochondrial DNA. *Nat. Genet.* **23**, 147–147 (1999).
- Devi, L., Raghavendran, V., Prabhu, B. M., Avadhani, N. G. & Anandatheerthavada, H. K. Mitochondrial import and accumulation of alpha-synuclein impair complex I in human dopaminergic neuronal cultures and Parkinson disease brain. *J. Biol. Chem.* **283**, 9089–9100 (2008).
- Franco-Iborra, S. et al. Defective mitochondrial protein import contributes to complex I-induced mitochondrial dysfunction and neurodegeneration in Parkinson's disease. *Cell Death Dis.* **9**, 1122–17 (2018).
- Thakur, P. et al. Modeling Parkinson's disease pathology by combination of fibril seeds and  $\alpha$ -synuclein overexpression in the rat brain. *Proc. Natl Acad. Sci. USA* **114**, E8284–E8293 (2017).
- Rocha, E. M. et al. Glucocerebrosidase gene therapy prevents  $\alpha$ -synucleinopathy of midbrain dopamine neurons. *Neurobiol. Dis.* **82**, 495–503 (2015).
- Volpicelli-Daley, L. A. et al. Exogenous  $\alpha$ -synuclein fibrils induce Lewy body pathology leading to synaptic dysfunction and neuron death. *Neuron* **72**, 57–71 (2011).
- Rocha, E. M., De Miranda, B. & Sanders, L. H. Alpha-synuclein: pathology, mitochondrial dysfunction and neuroinflammation in Parkinson's disease. *Neurobiol. Dis.* **109**, 249–257 (2017).
- Hsu, L. J. et al.  $\alpha$ -Synuclein promotes mitochondrial deficit and oxidative stress. *Am. J. Pathol.* **157**, 401–410 (2000).

11. Smith, W. W. et al. Endoplasmic reticulum stress and mitochondrial cell death pathways mediate A53T mutant alpha-synuclein-induced toxicity. *Hum. Mol. Genet.* **14**, 3801–3811 (2005).
12. Grassi, D. et al. Identification of a highly neurotoxic  $\alpha$ -synuclein species inducing mitochondrial damage and mitophagy in Parkinson's disease. *Proc. Natl Acad. Sci. USA* **115**, E2634–E2643 (2018).
13. Theodore, S., Cao, S., McLean, P. J. & Standaert, D. G. Targeted overexpression of human alpha-synuclein triggers microglial activation and an adaptive immune response in a mouse model of Parkinson disease. *J. Neuropathol. Exp. Neurol.* **67**, 1149–1158 (2008).
14. St Martin, J. L. et al. Dopaminergic neuron loss and up-regulation of chaperone protein mRNA induced by targeted over-expression of alpha-synuclein in mouse substantia nigra. *J. Neurochem.* **100**, 1449–1457 (2007).
15. Di Maio, R. et al. LRRK2 activation in idiopathic Parkinson's disease. *Sci. Transl. Med.* **10**, eaar5429 (2018).
16. Zharikov, A. D. et al. shRNA targeting  $\alpha$ -synuclein prevents neurodegeneration in a Parkinson's disease model. *J. Clin. Invest.* **125**, 2721–2735 (2015).
17. Liu, F.-T. et al. Involvement of mortalin/GRP75/mthsp70 in the mitochondrial impairments induced by A53T mutant  $\alpha$ -synuclein. *Brain Res.* **1604**, 52–61 (2015).
18. Higgins, D. S. & Greenamyre, J. T. [3H]dihydroxyrotenone binding to NADH: ubiquinone reductase (complex I) of the electron transport chain: an autoradiographic study. *J. Neurosci.* **16**, 3807–3816 (1996).
19. Testa, C. M., Sherer, T. B. & Greenamyre, J. T. Rotenone induces oxidative stress and dopaminergic neuron damage in organotypic substantia nigra cultures. *Mol. Brain Res.* **134**, 109–118 (2005).
20. De Miranda, B. R., Fazzari, M., Rocha, E. M., Castro, S. & Greenamyre, J. T. Sex differences in rotenone sensitivity reflect the male-to-female ratio in human Parkinson's disease incidence. *Toxicol. Sci.* **354**, 319 (2019).
21. Cannon, J. R. et al. A highly reproducible rotenone model of Parkinson's disease. *Neurobiol. Dis.* **34**, 279–290 (2009).
22. Rocha, E. M. et al. LRRK2 inhibition prevents endolysosomal deficits seen in human Parkinson's disease. *Neurobiol. Dis.* **134**, 104626 (2019).
23. Roberts, R. F., Bengoa-Vergniory, N. & Alegre-Abarrategui, J. Alpha-Synuclein proximity ligation assay (AS-PLA) in brain sections to probe for alpha-synuclein oligomers. *Methods Mol. Biol.* **1948**, 69–76 (2019).
24. Barrett, P. J. & Timothy Greenamyre, J. Post-translational modification of  $\alpha$ -synuclein in Parkinson's disease. *Brain Res.* **1628**, 247–253 (2015).
25. Copeland, W. C. & Longley, M. J. Mitochondrial genome maintenance in health and disease. *DNA Repair* **19**, 190–198 (2014).
26. Omura, T. Mitochondria-targeting sequence, a multi-role sorting sequence recognized at all steps of protein import into mitochondria. *J. Biochem.* **123**, 1010–1016 (1998).
27. Wiedemann, N., Frazier, A. E. & Pfanner, N. The protein import machinery of mitochondria. *J. Biol. Chem.* **279**, 14473–14476 (2004).
28. Honrath, B. et al. Glucose-regulated protein 75 determines ER-mitochondrial coupling and sensitivity to oxidative stress in neuronal cells. *Cell Death Discov.* **3**, 17076–13 (2017).
29. Jin, J. et al. Proteomic identification of a stress protein, mortalin/mthsp70/GRP75: relevance to Parkinson disease. *Mol. Cell Proteom.* **5**, 1193–1204 (2006).
30. Singh, A. P. et al. Serum mortalin correlated with  $\alpha$ -synuclein as serum markers in Parkinson's disease: a pilot study. *Neuromol. Med.* **20**, 83–89 (2018).
31. Burbulla, L. F. et al. Mitochondrial proteolytic stress induced by loss of mortalin function is rescued by Parkin and PINK1. *Cell Death Dis.* **5**, e1180–e1180 (2014).
32. Basso V, Marchesan E, Ziviani E. A trio has turned into a quartet: DJ-1 interacts with the IP3R-Grp75-VDAC complex to control ER-mitochondria interaction. *Cell Calcium*. **87**, 102186 (2020). <https://doi.org/10.1016/j.ceca.2020.102186>. Epub 2020 Feb 24.
33. Bose, A. & Beal, M. F. Mitochondrial dysfunction in Parkinson's disease. *J. Neurochemistry* **139**, 216–231 (2016).
34. Greenamyre, J. T., MacKenzie, G., Peng, T.-I. & Stephens, S. E. Mitochondrial dysfunction in Parkinson's disease. *Biochem. Soc. Symp.* **66**, 85–97 (1999).
35. Kowalska, M., Piekut, T., Prendecki, M., Sodel, A., Kozubski, W. & Dorszewska, J. Mitochondrial and Nuclear DNA Oxidative Damage in Physiological and Pathological Aging. *DNA Cell Biol* **39**, 1410–1420 (2020).
36. Giannoccaro, M. P., La Morgia, C., Rizzo, G. & Carelli, V. Mitochondrial DNA and primary mitochondrial dysfunction in Parkinson's disease. *Mov. Disord.* **32**, 346–363 (2017).
37. Sanders, L. H. et al. Mitochondrial DNA damage: molecular marker of vulnerable nigral neurons in Parkinson's disease. *Neurobiol Dis.* **70**, 214–223 (2014).
38. Gombash, S. E. et al. Morphological and behavioral impact of AAV2/5-mediated overexpression of human wildtype alpha-synuclein in the rat nigrostriatal system. *PLoS ONE*. **8**, e81426 (2013).
39. Altun, M., Bergman, E., Edström, E., Johnson, H. & Ulfhake, B. Behavioral impairments of the aging rat. *Physiol. Behav.* **92**, 911–923 (2007).
40. Reeve, A., Simcox, E. & Turnbull, D. Ageing and Parkinson's disease: why is advancing age the biggest risk factor? *Ageing. Res. Rev.* **14**, 19–30 (2014).
41. Van Laar, V. S. et al.  $\alpha$ -Synuclein amplifies cytoplasmic peroxide flux and oxidative stress provoked by mitochondrial inhibitors in CNS dopaminergic neurons in vivo. *Redox Biol.* **37**, 101695 (2020).
42. Surmeier, D. J. Determinants of dopaminergic neuron loss in Parkinson's disease. *FEBS J.* **285**, 3657–3668 (2018).
43. Pozo Devoto, V. M. & Falzone, T. L. Mitochondrial dynamics in Parkinson's disease: a role for  $\alpha$ -synuclein? *Dis. Model Mech.* **10**, 1075–1087 (2017).
44. Woodlee, M. T., Kane, J. R., Chang, J., Cormack, L. K. & Schallert, T. Enhanced function in the good forelimb of hemi-parkinson rats: compensatory adaptation for contralateral postural instability? *Exp. Neurol.* **211**, 511–517 (2008).
45. Tapias, V., Greenamyre, J. T. & Watkins, S. C. Automated imaging system for fast quantitation of neurons, cell morphology and neurite morphometry in vivo and in vitro. *Neurobiol. Dis.* **54**, 158–168 (2013).
46. Tapias, V. & Greenamyre, J. T. A rapid and sensitive automated image-based approach for in vitro and in vivo characterization of cell morphology and quantification of cell number and neurite architecture. *Curr. Protoc. Cytom.* **68**, 12.33.1–22 (2014).
47. De Miranda, B. R. et al. Astrocyte-specific DJ-1 overexpression protects against rotenone-induced neurotoxicity in a rat model of Parkinson's disease. *Neurobiol. Dis.* **115**, 101–114 (2018).

## ACKNOWLEDGEMENTS

This work was supported by research grants from the National Institutes of Health (NS100744, R21ES027470, NS095387, and K99ES029986), the American Parkinson Disease Association, the Parkinson's Foundation, the Michael J Fox Foundation, the Blechman Foundation, and the friends and family of Sean Logan.

## AUTHOR CONTRIBUTIONS

J.T.G. and B.R.D. designed the research; B.R.D., S.L.C., and E.M.R.; collected and analyzed the data. B.R.D. and J.T.G. interpreted the data and wrote the manuscript; J.T.G. and E.M.R. reviewed the manuscript.

## COMPETING INTERESTS

The authors declare no competing interests.

## ADDITIONAL INFORMATION

**Supplementary information** is available for this paper at <https://doi.org/10.1038/s41531-020-00139-6>.

**Correspondence** and requests for materials should be addressed to J.T.G.

**Reprints and permission information** is available at <http://www.nature.com/reprints>

**Publisher's note** Springer Nature remains neutral with regard to jurisdictional claims in published maps and institutional affiliations.



**Open Access** This article is licensed under a Creative Commons Attribution 4.0 International License, which permits use, sharing, adaptation, distribution and reproduction in any medium or format, as long as you give appropriate credit to the original author(s) and the source, provide a link to the Creative Commons license, and indicate if changes were made. The images or other third party material in this article are included in the article's Creative Commons license, unless indicated otherwise in a credit line to the material. If material is not included in the article's Creative Commons license and your intended use is not permitted by statutory regulation or exceeds the permitted use, you will need to obtain permission directly from the copyright holder. To view a copy of this license, visit <http://creativecommons.org/licenses/by/4.0/>.

© The Author(s) 2020